



## Article

# Analysis of Ecological Blockage Pattern in Beijing Important Ecological Function Area, China

Jiangqi Xu <sup>1,2</sup>, Jia Wang <sup>1,2,\*</sup>, Nina Xiong <sup>1,2</sup>, Yuhan Chen <sup>1,2</sup>, Lu Sun <sup>1,2</sup>, Yutang Wang <sup>1,2</sup> and Likun An <sup>1,2</sup>

<sup>1</sup> Institute of GIS, RS & GPS, Beijing Forestry University, Beijing 100083, China; xujiangqi@bjfu.edu.cn (J.X.); xiongnina@bjfu.edu.cn (N.X.); chenyu0228@bjfu.edu.cn (Y.C.); sunlu@bjfu.edu.cn (L.S.); yutangwang\_2020@bjfu.edu.cn (Y.W.); likun\_an@bjfu.edu.cn (L.A.)

<sup>2</sup> Beijing Key Laboratory of Precise Forestry, Beijing Forestry University, Beijing 100083, China

\* Correspondence: wangjia2009@bjfu.edu.cn; Tel.: +86-138-1066-4533

**Abstract:** With the implementation of human activities, such as logging, reclamation, and construction, the increasing fragmentation of ecological space and the increasing blockage of biological migration corridors cause many threats to biodiversity conservation. In this study, we used the Northwest Beijing Ecological Containment Area as the research area. Based on an integrated circuit theoretical model, we identified functional connectivity networks and analyzed the spatial and temporal changes of ecological blockage patterns in the region from 1998–2018 in terms of the landscape connectivity, ecological breakpoints, pinch points, and barriers, respectively. The results show that the average remote sensing ecological index had a trend of decreasing and then increasing, and a total of 33, 34, and 63 habitat core areas and 70, 74, and 152 ecological corridors were identified in 1998, 2010, and 2018, respectively. The regions with high ecological blockage were mainly in the central part of Yanqing District, the southwest corner of the study area, and the eastern urban area. Although the number of potential ecological corridors gradually increases with the probability of migration in the study area, the blockage status and vulnerability of the ecological corridors continue to increase due to the conflict between land uses. The ecological status of the study area reflects the comprehensive effectiveness of the capital's high-quality development under the strategic deployment of ecological civilization. In the context of habitat fragmentation, the effective protection and restoration of the ecological conditions in the ecological function areas is of great importance in guaranteeing the ecological quality and sustainable development of the country.

**Keywords:** circuit theory; remote sensing ecological index; ecological blockage; dynamic; land use; fragmentation



**Citation:** Xu, J.; Wang, J.; Xiong, N.; Chen, Y.; Sun, L.; Wang, Y.; An, L. Analysis of Ecological Blockage Pattern in Beijing Important Ecological Function Area, China. *Remote Sens.* **2022**, *14*, 1151.

<https://doi.org/10.3390/rs14051151>

Academic Editor: Georgios Mallinis

Received: 20 January 2022

Accepted: 23 February 2022

Published: 25 February 2022

**Publisher's Note:** MDPI stays neutral with regard to jurisdictional claims in published maps and institutional affiliations.



**Copyright:** © 2022 by the authors. Licensee MDPI, Basel, Switzerland. This article is an open access article distributed under the terms and conditions of the Creative Commons Attribution (CC BY) license (<https://creativecommons.org/licenses/by/4.0/>).

## 1. Introduction

Continued human activity alters the land use and land cover of a region, resulting in landscape fragmentation, which is considered to be a key driver for the loss of natural habitat, the spread of patches, and the reduction in biodiversity [1,2]. With population and economic growth, the human impact on the surface landscape, including the phenomenon of urban sprawl and the continued extension and networking of artificial corridors such as roads, has increased dramatically [3–5]. The meaning of ecological blockage in the ecological sense includes, in addition to geospatial distance blockage (geographic isolation), migration and blocked isolation of genetic exchange and movement among individuals or populations of organisms caused by changes in subsistence conditions, such as climate temperature, moisture, and food, as well as by shifts in land use types. Landscape connectivity is generally used to measure the degree of isolation of the gene flow by the landscape pattern [6]. Under the dual threats of climate change and the expansion of modified ecosystems, the protection and the restoration of landscape connectivity by creating effective ecological networks have become core strategies for nature conservation [7–9].

Landscape fragmentation changes the structural connectivity of a region that emphasizes the characteristics of landscape heterogeneity and is usually harmful to the natural and semi-natural environment [10,11]. It often affects critical ecosystem services and human health and creates obstacles to the ecological flow of native species [12–14]. In these contexts, fragmentation undoubtedly represents the basic element as a quantitative description of the landscape structure and organization. The landscape fragmentation process affects biodiversity in two main ways: the decrease in the area of habitat patches and the reinforcement in the isolation between patches [15,16]. The former mainly changes a series of microevolutionary processes by reducing local populations, such as by the bottleneck effect, inbreeding decline, random drift, etc. Additionally, the latter mainly leads to blockage of the gene flow between local populations, the weakening of the “rescue effect”, and even loss, increasing the risk of local extinction [17,18].

Studies have shown that changes in environmental gradients (e.g., topographic slope, elevation, moisture conditions, etc.), vegetation type, and community structure can significantly affect population dispersal routes and gene flow connectivity [19,20]. In contrast, studies on landscape fragmentation have also shown that linear landscape elements (e.g., highways) exhibit a significant segregation of the genetic structure and gene flow for animal populations on both sides [21,22]. Previously, the distance isolation model based on linear distance (IBD) was generally used as the null model to analyze the least-cost path of gene flow [23]. However, the adaptability of this metric is limited and does not reflect the full range of biological transport processes [24]. Later, McRae proposed the concept of isolation-by-resistance to integrate the isolation effects of space, environment, and landscape [25]. Since 2006, McRae et al. have introduced circuit theory to the field of ecology and conservation biology through a series of seminal papers [12,25,26]. Circuit theory has been widely used in biodiversity conservation research, both domestically and internationally, due to the theory’s innovative provision of a process-driven model to simulate gene flow and the movement of organisms in heterogeneous landscapes that is stable at a variety of scales [27–32]. Circuit theory can identify all the potential ecological corridors available for species or ecological processes within the landscape and extends the identification of pinch points, barrier areas, etc. [29]. Meanwhile, the widely used connectivity measurement method is the least-cost path (LCP), based on the resistance plane. The LCP is an excellent model for measuring functional connectivity despite its inherent drawbacks: it only simulates the path with the least accumulated resistance, but only considering the diffusion of a single optimal path will underestimate the impact of habitat fragmentation on the connectivity between populations or patches because local fragmentation may not affect the optimal path, but it may, rather, reduce the overall quality of the landscape [33–35]. The combined application of the two techniques for building ecological networks and restoring connections between isolated patches can complement each other and help to better reflect the migratory exchange of organisms in heterogeneous landscapes as well as the barriers [27,30]. In addition, the construction methods of resistance planes in circuit theory and the least-cost path are similar and have better compatibility when combining the two models.

During the “Eleventh Five-Year Plan” period, Beijing planned to form four major urban function areas and put forward the concept of the “ecological connotation development area”. In the same period, the “Beijing Urban Master Plan (2004–2020)” clearly proposed the functional area of the “Northwest Ecological Containment Area”. The new “Beijing Urban Master Plan (2016–2035)” further defines this area as the ecological development guarantee area and the comprehensive service center in northwest Beijing, which is the key area for guaranteeing the sustainable development of the capital. In recent years, with the rapid population and economic growth and ecological construction, the land use status of the Northwest Beijing Ecological Containment Area (NBCECA) has changed dramatically, and the ecosystem pattern has changed significantly. It is important to assess the degree of damage to the ecological space and ecological functions and to analyze the impact of the fragmentation changes presented by the habitat sites. Although Chinese scholars have

gradually carried out some studies on the ecological cultured areas [36–38], there are still relatively few relevant studies, especially on ecological network protection and restoration, for which there is no relevant literature; thus, it is of great significance to evaluate the status of the ecological function blockage in the NBECA. There are many mature studies on ecological networks and ecological integrity restoration [39–43], but most of them are based on single-period analysis of ecological conditions. They provide restoration suggestions but less on the overall evolution of ecological patterns in a long time series.

In this paper, we take the NBECA as the study area and select three phases of remote sensing images to calculate the remote sensing ecological index (RSEI) for ecological quality evaluation, with the integration of the importance of the patches in identifying core habitat areas. Ecological resistance surfaces were constructed by selecting factors such as land use types, habitat quality, slope, elevation, water density, road density, population density, and mining site density. Based on the Circuitscape platform and Linkage mapper software, we aim to analyze the spatial and temporal changes of the ecological blockage with habitat fragmentation in the northwest cultured area of Beijing over the past 20 years. We expect to provide an ecological planning basis for biodiversity conservation and nature reserve management in Beijing and to provide a reference scheme for planning managers in the ecological protection and restoration of an important ecological function area (IEA).

## 2. Materials and Methods

### 2.1. Study Area

The Northwest Beijing Ecological Containment Area (NBECA) is an important ecological function area in the Beijing-Tianjin-Hebei region, as well as an important ecological security barrier and water connotation area and a key area for guaranteeing the ecological environment quality and sustainable development of the capital, Beijing (Figure 1). The research area is located at 115°24′57″~116°20′42″E, 39°30′20″~40°37′44″N, with a total area of 5185 km<sup>2</sup>, covering the whole district of Mentougou, most areas of Fangshan, Yanqing, Changping, and Shijingshan, as well as the local areas of Haidian and Fengtai. Its climate belongs to the mid-latitude continental monsoon climate, and the climate difference between the western mountainous area and the eastern plain is obvious, with an average annual temperature of 8 °C–19 °C. Precipitation in the region is focused on the period from June to September, with an average annual rainfall of about 555 mm and the highest annual rainfall of 630 mm in the area of Xiayunling in Fangshan District. The topography of the study area is predominantly mountainous, with the highest point located at Ling Mountain in the northwestern part of Mentougou District at an elevation of 2287 m.

The study area is rich in tree species, including natural oil pine forest, larch, birch, etc., and spans the Chaobai River, the Yongding River, and the Rejected River basins. The Yongding River runs through the entire study area, and the rich climatic diversity and habitat diversity nurtures a rich diversity of wildlife. There are a large number of forest parks, wetlands, important wind and sand management areas, and nature reserves in the study area, including two national nature reserves, Songshan and Baihuashan. According to the Beijing Statistical Yearbook 2018, the population in the study area was about 1.42 million at the end of 2017. Furthermore, the population density increases from the mountainous area in the northwest to the plain area in the southeast. It is crucial to solve the contradiction between the protection of the ecological environment and the economic development and to establish the compensation mechanism for ecological construction benefits.

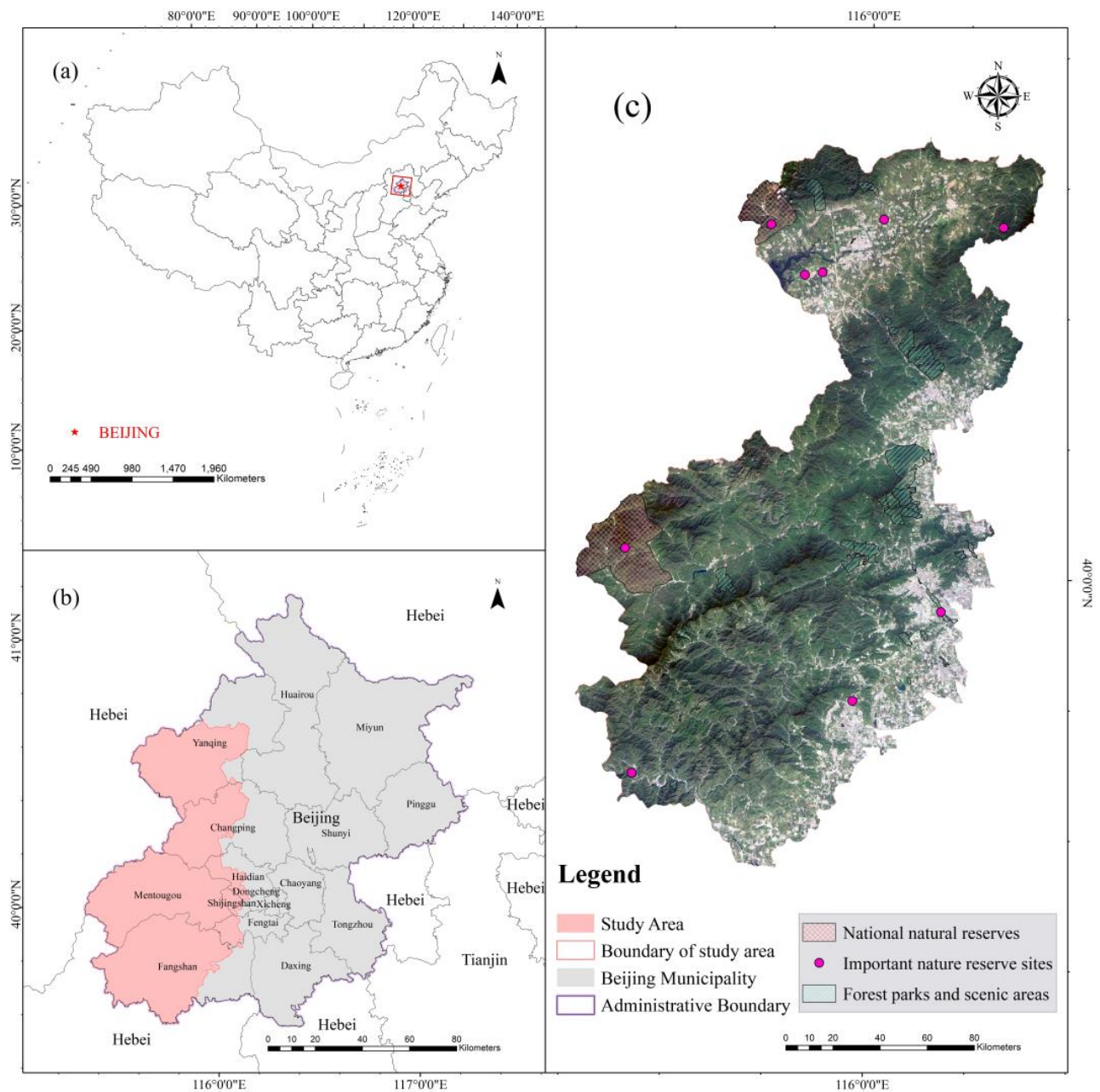


**Figure 1.** Geographic location of study area: (a) in China and (b) in Beijing. (c) The remote sensing image of study area.

## 2.2. Data Sources and Processing

The data used in this study are as follows: (1) the land cover data of 5 m resolution in 1998, 2010, and 2018 and the vector boundary of the study area were all obtained from the Beijing Municipal Science and Technology Project “Research on the Technical Methodology of Investigation and Assessment of Damaged Ecological Space and Ecological Integrity Restoration in Northwest Cultural Area”. The land cover data were obtained with an accuracy of more than 85%, which could be used in this research. The main land use types obtained were water body, arbor forest, shrubland, grassland, cropland, bare ground, built area, gravel pit, and ore heap (Figure 2). (2) The socio-economic, demographic and climatic data were obtained from the statistical yearbook information of each district in Beijing and the related literature. (3) The administrative zoning map data were obtained from the Geospatial Data Cloud. (4) The DEM data are raster map with a 90 m resolution from

the Data Center for Resource and Environmental Sciences, Chinese Academy of Sciences. In addition, the slope map of the study area was calculated in ArcGIS 10.6 using the digital elevation model. (5) The water density data and mining site density data of the study area for 1998, 2010, and 2018 were obtained based on land cover data through the Kernel Density module in ArcGIS 10.6 software. (6) The road network data were obtained from the Peking University data platform. The road density data were also obtained through the Kernel Density module. (7) The population density data were from the high-precision Worldpop population density database: 2000–2020 Chinese population density dataset. The unit is the level of population per square kilometer, and the spatial reference system is the geographic coordinate system WGS 84 with a spatial resolution of 100 m [44]. (8) The spatial distribution of the nature conservation sites is from OpenStreetMap. The details of the data sources used in the study are shown in Table 1.

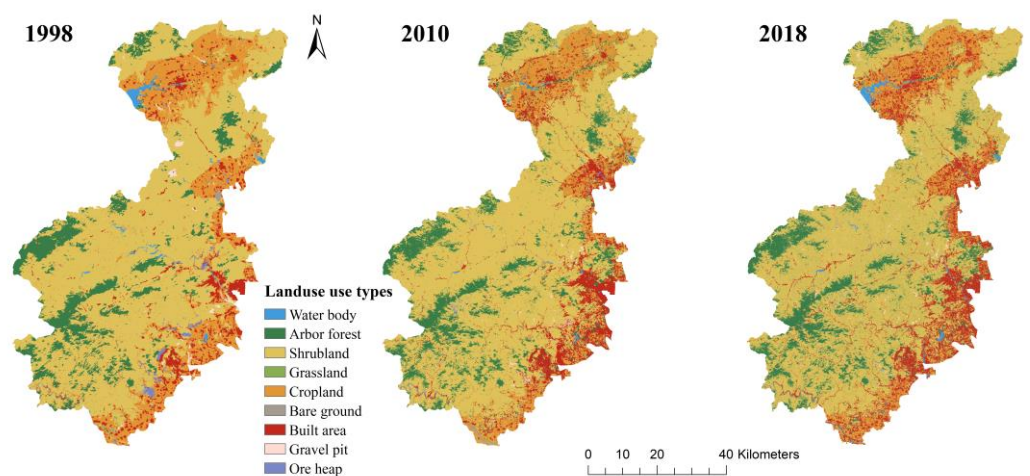


**Figure 2.** Land use types of the study area in 1998, 2010, and 2018.

**Table 1.** Datasets used in this study.

Data	Data Type	Resolution	Data Source
Land cover data	Raster	5 m	Beijing Municipal Science and Technology Project (Z181100005318003)
Vector boundary of the study area	Vector	-	
Socio-economic, demographic, and climatic data	Statistical	-	Yearbook data, etc.
Administrative zoning map	Vector	-	Geospatial data cloud ( <a href="http://www.gscloud.cn">http://www.gscloud.cn</a> , accessed on 30 July 2021)
DEM data	Raster	90 m	Data Center for Resource and Environmental Sciences, Chinese Academy of Sciences ( <a href="http://www.resdc.cn">http://www.resdc.cn</a> , accessed on 12 April 2021)
Road network data	Vector	-	Beijing University Data Platform ( <a href="http://geodata.pku.edu.cn">http://geodata.pku.edu.cn</a> , accessed on 30 July 2021)
Population density data	Raster	100 m	High precision Worldpop population density dataset ( <a href="http://www.worldpop.org">http://www.worldpop.org</a> , accessed on 30 July 2021)

### 2.3. Methods

#### 2.3.1. Remote Sensing Ecological Index

In this study, the remote sensing ecological index (RSEI) created by Hanqiu Xu [45] was used to evaluate the habitat quality in the study area, which consists of the normalized vegetation index (NDVI), the wetness component of the tasseled cap transformation (WET), and the land surface temperature (LST) and the normalized difference built-up and soil

index (NDBSI), coupled to reflect the greenness, wetness, heat, and dryness that are closely related to human activities [46]. The index to assess the spatial and temporal variation of ecological quality has been widely used at different scales [47–49]. In recent years, some researchers have started to apply it to ecological network construction, and the validity and accuracy have been verified to some extent [50–52]. We calculated the index based on the Google Earth Engine platform and extracted the RSEI for 1998, 2010, and 2018 by processing such as de-clouding, water body masks, calculating indicators, overlaying to extract median values and mosaic, etc. The remote sensing data source used was Landsat TM/OLI images with a spatial resolution of 30 m (Table 2). All the image data were selected from the summer season (June–September) to avoid the influence of seasonal differences.

**Table 2.** The details of Landsat images.

Target Year	1998	2010	2018
Sources	Google Earth Engine		
Number of image views	21	21	27
Datasets	Landsat 5 TM datasets 1984–2012 (30 m)	Landsat 8 OLI and TIRS datasets 2013–2018 (30 m)	
Name	LANDSAT/LT05/C02/T1_L2	LANDSAT/LC08/C02/T1_L2	
Description	Surface reflectance data		
Season	Summer (June–September)		

### (1) Calculation of greenness index

The normalized vegetation index is undoubtedly the most widely used vegetation index, which is closely related to plant biomass, leaf area index, and vegetation cover. It is calculated as follows [49]:

$$NDVI = \frac{\rho_{NIR} - \rho_{red}}{\rho_{NIR} + \rho_{red}} \quad (1)$$

where NDVI is the normalized vegetation index of the study area.  $\rho_{red}$  and  $\rho_{NIR}$  are, respectively, the reflectivity of the red band and the near-infrared band corresponding to the TM image and the OLI image.

### (2) Calculation of wetness index

The wetness component reflects the moisture content of water bodies and soil and vegetation, which is closely related to ecology. The wetness is calculated as follows [49]:

$$WET_{(TM)} = 0.0315\rho_{blue} + 0.2021\rho_{green} + 0.3102\rho_{red} + 0.1594\rho_{NIR} - 0.6806\rho_{SWIR1} - 0.6109\rho_{SWIR2} \quad (2)$$

$$WET_{(OLI)} = 0.1511\rho_{blue} + 0.1972\rho_{green} + 0.3283\rho_{red} + 0.3407\rho_{NIR} - 0.7117\rho_{SWIR1} - 0.4559\rho_{SWIR2} \quad (3)$$

where WET is the surface moisture index.  $\rho_{blue}$ ,  $\rho_{green}$ ,  $\rho_{red}$ ,  $\rho_{NIR}$ ,  $\rho_{SWIR1}$ , and  $\rho_{SWIR2}$  are, respectively, the reflectivity of the ground objects in the blue, green, red, near-infrared, short-wave infrared 1, and short-wave infrared 2 bands corresponding to the TM image and the OLI image.

### (3) Calculation of heat index

In this study, the inverse surface temperature was used to characterize the heat index. The calculation equation is shown below [49]:

$$LST = A_i \frac{T_b}{\varepsilon} + B_i \frac{1}{\varepsilon} + C_i \quad (4)$$

$$\begin{cases} \varepsilon_{\text{water}} = 0.995 \quad (\text{NDVI} \leq 0) \\ \varepsilon_{\text{building}} = 0.9589 + 0.086 \times F_{\text{veg}} - 0.0671 \times F_{\text{veg}}^2 \quad (0 < \text{NDVI} < 0.7) \\ \varepsilon_{\text{natural}} = 0.9625 + 0.0614 \times F_{\text{veg}} - 0.0461 \times F_{\text{veg}}^2 \quad (\text{NDVI} \geq 0.7) \end{cases} \quad (5)$$

where LST is the surface temperature index.  $T_b$  is the reflection value of the top atmosphere of the TIRS channel,  $\varepsilon$  is the surface emissivity, and the coefficients  $A_i$ ,  $B_i$ , and  $C_i$  are determined by linear regression. It is the radiation transmission simulation of 10 types of TCWV ( $i = 1, \dots, 10$ ) [53].  $F_{\text{veg}}$  represents the vegetation coverage.

#### (4) Calculation of dryness index

The dryness index can be synthesized from both the surface bare soil index SI and the surface building index IBI [49]:

$$\text{NDBSI} = \frac{\text{SI} + \text{IBI}}{2} \quad (6)$$

$$\text{SI} = \frac{(\rho_{\text{SWIR1}} + \rho_{\text{red}}) - (\rho_{\text{blue}} + \rho_{\text{NIR}})}{(\rho_{\text{SWIR1}} + \rho_{\text{red}}) + (\rho_{\text{blue}} + \rho_{\text{NIR}})} \quad (7)$$

$$\text{IBI} = \frac{2\rho_{\text{SWIR2}}/(\rho_{\text{SWIR1}} + \rho_{\text{NIR}}) - \left[ \rho_{\text{NIR}}/(\rho_{\text{red}} + \rho_{\text{NIR}}) + \rho_{\text{green}}/(\rho_{\text{SWIR1}} + \rho_{\text{green}}) \right]}{2\rho_{\text{SWIR2}}/(\rho_{\text{SWIR1}} + \rho_{\text{NIR}}) + \left[ \rho_{\text{NIR}}/(\rho_{\text{red}} + \rho_{\text{NIR}}) + \rho_{\text{green}}/(\rho_{\text{SWIR1}} + \rho_{\text{green}}) \right]} \quad (8)$$

where NDBSI is the dryness index of the study area.  $\rho_{\text{blue}}$ ,  $\rho_{\text{green}}$ ,  $\rho_{\text{red}}$ ,  $\rho_{\text{NIR}}$ ,  $\rho_{\text{SWIR1}}$ , and  $\rho_{\text{SWIR2}}$  are, respectively, the reflectivity of the ground objects in the blue band, green band, red band, near-infrared band, short-wave infrared 1 band, and short-wave infrared 2 band corresponding to the TM image and OLI image.

#### (5) Construction of comprehensive ecological index

Finally, the range of standardized removal dimensions is adopted for a single index, and the remote sensing ecological index is constructed according to the principal component transformation (Equation (9)) [49].

$$\text{RSEI} = \text{PCA}[f(\text{NDVI}, \text{WET}, \text{NDBSI}, \text{LST})] \quad (9)$$

To facilitate comparison, we standardize the RSEI to [0, 1] and divide the RSEI into the five levels of low (0–0.2), lower (0.2–0.4), medium (0.4–0.6), higher (0.6–0.8), and high (0.8–1.0) [54].

### 2.3.2. Circuit Theory

Circuit theory combines circuitry in physics with ecology through random walk theory, where the landscape is treated as a conductive surface during species migration or dispersal, with high permeability landscapes having low resistance and low permeability landscapes having high resistance [27]. The circuit theory combined with the random walk theory gives the model more explanatory power by identifying multiple diffusion paths with a certain width, showing corridor redundancy and determining the relative importance of habitat patches and corridors by the strength of the currents between the source sites [12,25,26]. At the same time, the circuit theory simulated corridor can meet the demand of multi-species migration, which is more in line with the real situation of species movement and can be used for conservation planning and predicting the ecological and genetic effects of spatial heterogeneity and landscape change [24,32]. The physical terms and explicit ecological meanings associated with the circuit theory model are listed in Table S1. See more in Supplementary Materials.

#### 1. Simulation of circuit connectivity

In this paper, we used Circuitscape 5.0 [55] software to identify the potential corridor distributions by simulating species migration paths or gene flow. The current density values (the magnitude of the current through a single image element) obtained from the simulations characterize the probability values of organisms passing through the area as

they move between ecological node patches. Circuit theory complements the least-cost path approaches because it considers the effects of all the possible pathways across a landscape simultaneously [25,26]. The current density values for the entire study area, obtained by running Circuitscape 5.0 in Julia pairwise model calculations, provide a more intuitive picture of the overall connectivity of the area and where it is constrained.

## 2. Identification of ecological break points

Meanwhile, based on the circuit theory, we used the Linkage Mapper plug-in tools of ArcGIS to extract the path with the least resistance to connect two ecological source sites as ecological corridors [56]. Ecological corridors are bridges between ecological sources and low-resistance ecological channels for ecological flows between neighboring ecological sources. The Linkage Pathways tool is used to map the linkages among “core areas” of habitat on a landscape. First, we calculate the cost-weighted distance (CWD) of all pixels on the integrated ecological resistance surface to the source. The cost-weighted distance (CWD) of all the pixels on the integrated ecological resistance surface to the source is created, and then, the CWD grid is overlaid with the source to calculate the cumulative cost paths between sources. The least-cost distance (LCD) is formed by the minimum value of the path, the corresponding paths are the least-cost path (LCP), and finally, the critical corridors and potential corridors are obtained. Large traffic roads affect landscape fragmentation and cause blockage to ecological corridors; thus, we overlaid the traffic road map with the ecological corridor map for analysis to identify the ecological breakpoint areas.

## 3. Identification of ecological pinch points and barriers

The Linkage Mapper tools also allow for the identification and analysis of source site centrality, corridor “pinch points”, and barrier areas in landscape connectivity. Based on the minimum cost corridor extracted by Linkage Pathways, we set the “width” of the ecological corridor to 50,000 [29,57] in order to facilitate the calculation and better display the pinch points in the corridor. We used the Centrality Mapper [58] tool and the Pinchpoint Mapper [59] tool to analyze centrality and identify the pinch point areas within the minimum cost corridor by running the Circuitscape program. Centrality can be used to quantify the importance of the core areas and least-cost paths in maintaining the overall connectivity of the corridor network system [58]. The pinch point (a.k.a. bottlenecks or choke points) area between adjacent habitats represents a “bottleneck” area affecting the corridor between two adjacent habitats and is important for maintaining corridor connectivity. We also used the Barrier Mapper [60] tool to detect the important obstacles that affect the flow of the corridor. Ecological barrier areas are areas of high resistance to species movement between source sites, and their removal can improve connectivity between source sites and enhance species migration success [60]. The areas with high improvement scores can be rehabilitated to improve multiple corridors in the study area.

### 2.3.3. Grid Analysis Method

In this paper, we used grid analysis to divide the NBECA into grids with 1 km × 1 km grid measurement cells. Additionally, based on the land cover data, we calculated the landscape fragmentation index for each grid using Fragstats 4.2 software and the zoning statistics tool in ArcGIS. The landscape fragmentation index ( $F_i$ ) is calculated as follows:

$$F_i = \frac{N_i}{A_i} \quad (10)$$

where  $A_i$  is the area of the landscape component,  $N_i$  is the number of patches, and  $i$  is the certain land use type. Meanwhile, we used the zoning statistics tool in ArcGIS 10.6 to extract the average fragmentation index of each grid of the ecological corridor.

### 2.3.4. Creation of a Landscape Resistance Layer

The absolute size of the resistance value does not have a significant effect on landscape connectivity for the same type of assignment [61]. We assign five levels of resistance values,

with resistance values of 1, 250, 500, 750, and 1000 [35,61]. The higher the resistance value, the greater the ecological resistance, which is less conducive to the flow of information between species. Combining the natural background of the study area, we selected eight natural or human factors, such as land use, elevation, slope, RSEI, water density, population density, road density, and mining site density to construct the resistance surface from the sensitivity and risk considerations. The forests and the water sources have high ecological service value in the region; not only do they have high ecological quality, but they also play an important role in regional material and energy circulation [51]. The selection of areas with high ecological services and suitable habitats for species as ecological source sites will enable the ecological environment to develop in a healthy direction and to better serve the ecosystem. Mining and sandy areas are prone to many ecological problems, such as soil environmental damage and soil erosion, making their ecological service value the smallest and thus their resistance coefficient the largest compared to the other types [62]. The terrain factor classification is based on the distribution of vegetation types in the study area. Meanwhile, we use the natural interruption point method in ArcGIS 10.6 to reclassify, respectively, the water density factor, population density factor, road density factor, and mining site density factor. The resistance surface is analyzed uniformly at a landscape grain size of 30 m. For the setting of the resistance value weights, we have, on the one hand, based our results on the opinion of experts in this study area and, on the other hand, have referred to previous studies [51,52,62,63] (Table 3).

**Table 3.** Assignment table of resistance factors in the study area.

Aspect	Evaluation Factor	Resistance Value					Weights
		1	250	500	750	1000	
Natural Factors	Land use types	Water body, Arbor Forest	Shrubs, Grasslands	Cultivated land, Bare land	Building area	Gravel pit, Ore pile	0.3
	Elevation (m)	<500	500–800	800–1200	1200–1600	>1600	0.1
	Slope (°)	0–8	8–15	15–25	25–45	>45	0.1
	RESI = f (ndvi, wet, ndbsi, lst)	0.8–1	0.6–0.8	0.4–0.6	0.2–0.4	0–0.2	0.2
	Water source density	>200	100–200	50–100	10–50	<10	0.05
Human Factors	Mining site density	<50	50–300	300–1800	1800–5400	>5400	0.05
	Population density	0–10	10–50	50–100	100–200	>200	0.1
	Road density	0–1	1–3	3–5	5–10	>10	0.1

### 2.3.5. Selection of Habitat Core Areas

The habitat core area is generally located in the center of the nature reserve and is less subject to human interference, with rich wildlife resources and good ecological environment quality. Natural ecological patches in the landscape with better habitat quality are usually selected as ecological source sites. In this study, by using the 5 m spatial resolution land cover data decoded from remote sensing images and the calculated remote sensing ecological index, we selected, respectively, tree forests with an area larger than 1 km<sup>2</sup> and excellent habitat quality and more stable natural ecological patches of water bodies with an area larger than 1 km<sup>2</sup> as ecological nodes. Usually, the radiation range of fine-grained patches is limited; the 1 km<sup>2</sup> habitat patches are sufficient to cover the radiation range [51,62,63]. In addition, we used Circuitscape 5.0 software to combine the ecological nodes with the conductivity surfaces to perform all-to-one model operations

to obtain the relative importance size of the ecological patches. We used the natural interruption method to grade the obtained current density values and selected patches with greater importance (excluding those with the least degree of relative importance) and finally obtained, respectively, a total of 33, 34, and 63 patches as core habitat areas in 1998, 2010, and 2018. There were, respectively, 28, 30, and 59 arboreal woodland patches and 5, 4, and 4 water patches in the HCAs in 1998, 2010, and 2018. The number of patches in the HCAs showed an increasing trend during 1998–2018 (Figure 3), which was closely related to the increasing habitat quality in the study area on the one hand and influenced by the fragmentation of habitat patches on the other hand.

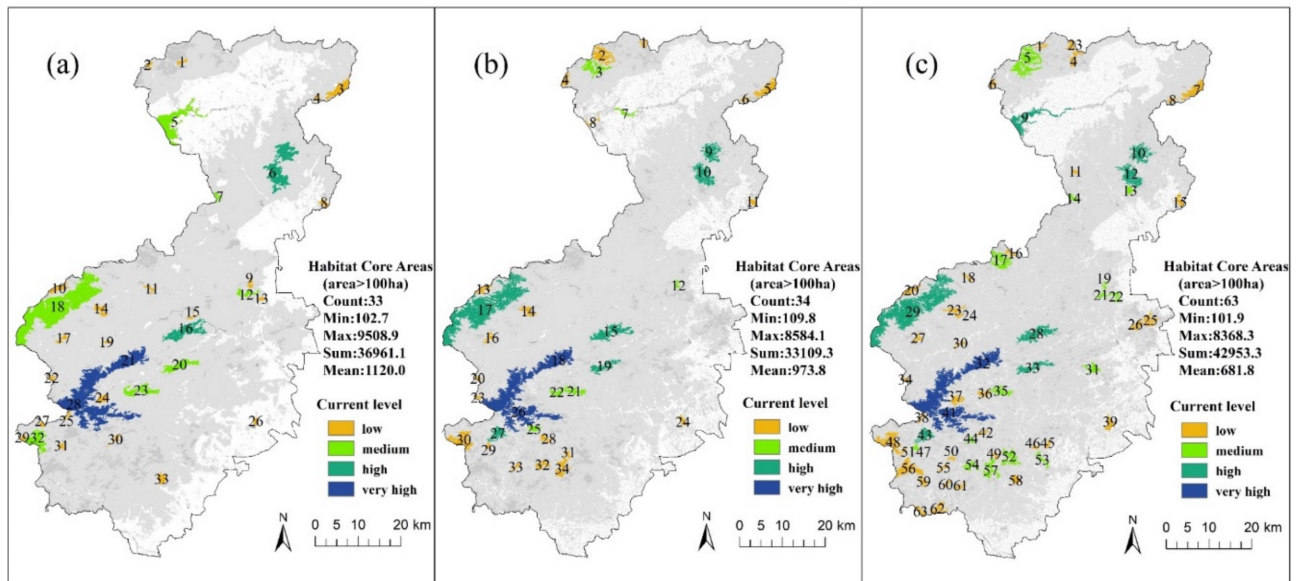


**Figure 3.** Selected habitat core areas of the study area and their importance level in (a) 1998; (b) 2010; and (c) 2018.

The increase in habitat core patches was mainly concentrated in the southwestern part of the study area, as well as the nature reserves and forest parks and wetland parks in the northwestern, central western, and eastern urban areas. It indicates that the nature reserves and forest parks, etc., have been effectively restored and protected, forest coverage has been improved, and the ecological environment quality has become significantly better with the increased protection efforts during 1998–2018. The changes in the scope of Baihuashan National Nature Reserve, Songshan National Nature Reserve, and Wild Duck Lake Wetland National Nature Reserve are particularly obvious, which indicates that the construction of nature reserves has positively contributed to the maintenance of the ecological circulation paths and the construction of the ecological spatial networks. The ecological red line in Beijing is a safety bottom line to protect ecological functions and environmental quality. The screening effect of habitat core areas is shown in the Table 4.

**Table 4.** Parameters of habitat core areas.

Year	1998	2010	2018
Number of patches	33	34	63
Areas (ha)	36,961.1	33,109.3	42,953.3
Percentage of redline area (%)	54.49	60.03	60.59

### 3. Results

#### 3.1. Spatio-Temporal Analysis of Ecological Quality Pattern

Among the correlation coefficients between the RSEI and each subindex, NDVI and WET were positively correlated with the RSEI, and the NDBSI and LST were negatively correlated with the RSEI, indicating that the larger the RSEI value, the better the ecological environment quality [48,49]. The ecological environment quality grades were classified into five grades of low [0–0.2], lower (0.2–0.4), medium (0.4–0.6), higher (0.6–0.8), and high (0.8–1), with 0.2, 0.4, 0.6, and 0.8 as intervals, based on the reference of related studies [45–49] and the Technical Specification of Ecological Environment Condition (HJ 192–2015). The evaluation results show that the average values of the remote sensing ecological index in 1998, 2010, and 2018 are 0.6538, 0.5862, and 0.7487, respectively. The mean values of the RSEI in the study area showed a brief downward trend during 1998–2010, followed by an increase during 2010–2018.

As can be seen from Figure 4, the areas with good ecological environment quality are mainly located in the western mountainous areas, with forested land as the main distribution type. The spatial distribution of habitat quality is consistent with the characteristics of woodland distribution and the topographic characteristics of the study area at three levels: the mountainous area, the plain area, and the urban construction area. It can be seen that the ecological quality of the study area is better in the western mountainous areas and worse in the plain urban areas such as Haidian District and Fengtai District. The results in Figure 4 show that the ecological degradation over the three years was more severe in 2010. As shown in the Table 5, the increase in the area of low-quality areas in 2010 compared to 1998 may be related to the urban expansion of the site and the increase in the area of built-up land, whereas the area of high-quality areas increased significantly in 2018.

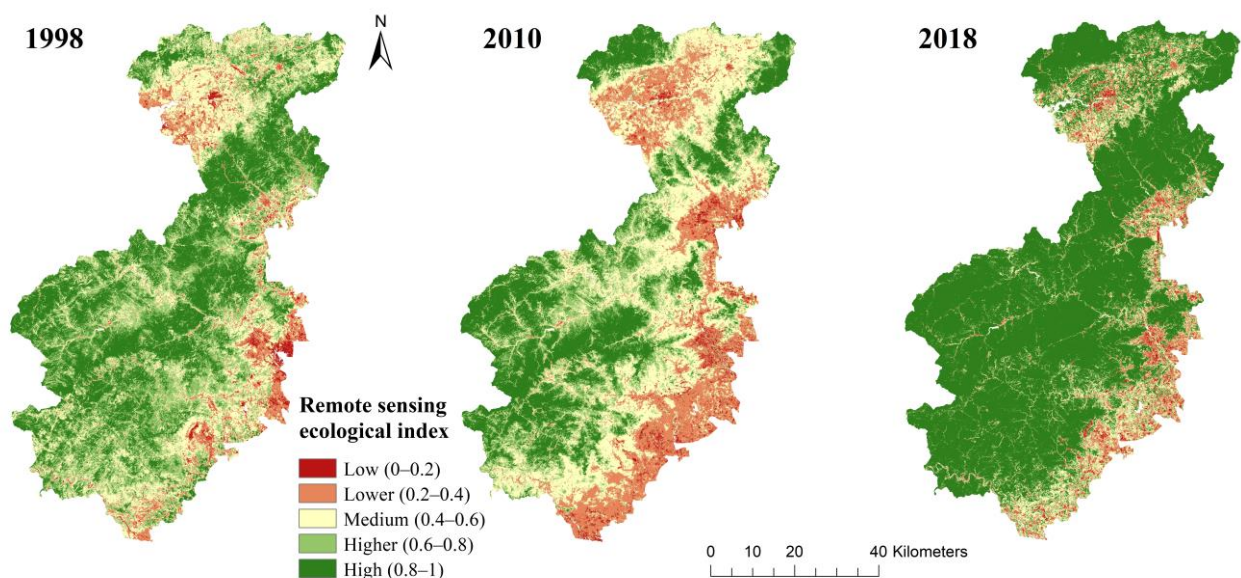


**Figure 4.** Ecological quality grade of the study area (1998–2018).

**Table 5.** Proportion of ecological quality of five grades in the study area from 1998 to 2010.

Level	RESI	Proportion of Different Quality Levels in Different Years (%)		
		1998	2010	2018
Low	(0–0.2)	1.84	2.17	1.90
Lower	(0.2–0.4)	9.13	18.85	7.35
Medium	(0.4–0.6)	26.01	32.80	12.66
Higher	(0.6–0.8)	28.27	18.27	5.65
High	(0.8–1.0)	34.75	27.90	72.44

Overall, the ecological environment quality in the northwest cultured area of Beijing has gradually improved in recent years with the managers' attention to the ecological environment and the adoption of relevant protection measures. However, individual places such as built-up areas, especially those with a high population density, have been subject to increasing environmental degradation due to interference from human activities.

### 3.2. Spatio-Temporal Analysis of Ecological Blockage Pattern

By analyzing the spatial and temporal evolution of the overall landscape connectivity in the study area with the use of the current density maps to reflect the migration probability between any two source sites, we found that the number and location of the habitat core areas played a dominant role in influencing the overall connectivity of the study area (Figure 5), and the magnitude of current values increased year by year from 1998 to 2018, which indicates that the landscape permeability became higher and the landscape matrix connectivity improved year by year. The great improvement in landscape connectivity in 2018 compared to 1998 and 2010 may be related to the national emphasis in recent years on the construction of ecological civilization. The ecological environment has been improved through effective management of nature reserves; for example, the improved ecological environment of Songshan National Nature Reserve, located in the upper northwest corner of Yanqing District, has led to enhanced connectivity above the study area in Figure 5.

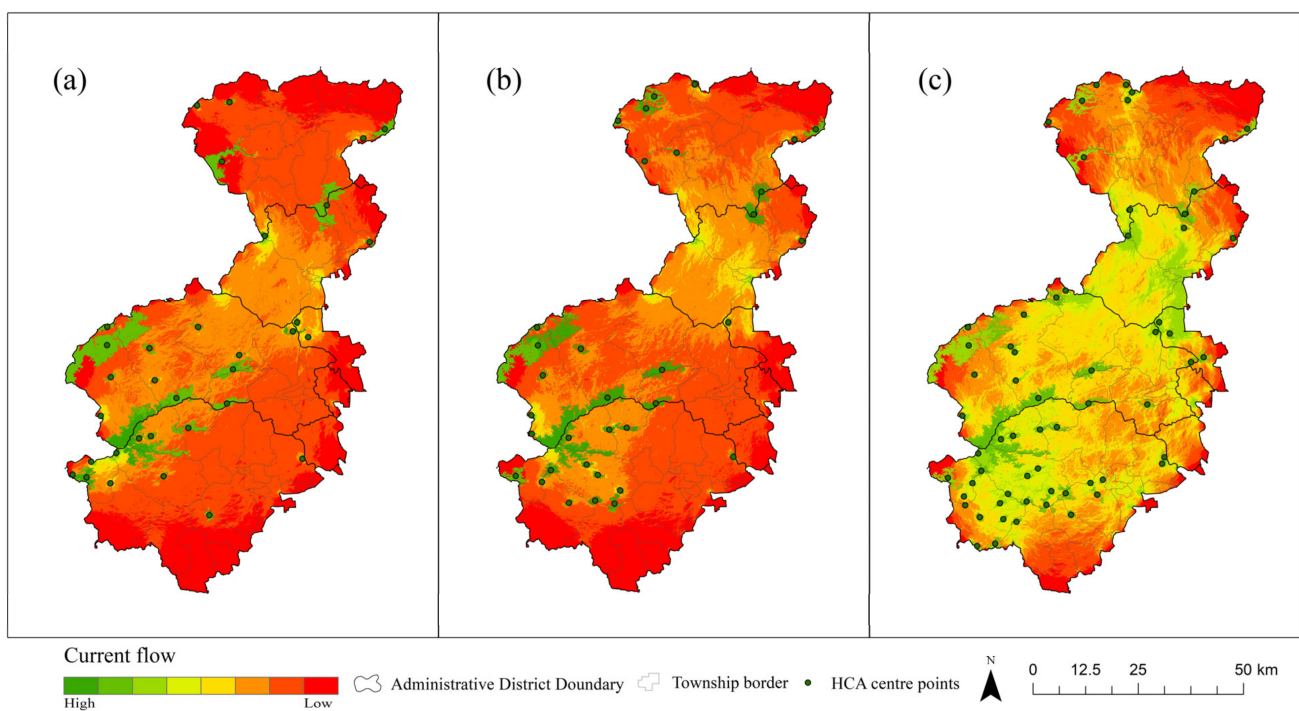


**Figure 5.** Maps of current flow based on circuit theory: (a) year 1998; (b) year 2010; and (c) year 2018. From top to bottom, the administrative districts are Yanqing, Changping, Haidian, Mentougou, Shijingshan, Fengtai, and Fangshan.

In 1998, more than 50% of the study area was dominated by low to very low current values (Figure 5a), implying that the mobility of organisms in the habitat landscape was greatly impeded. However, the areas with high ecological connectivity in 2018 make up most of the study area and are concentrated in the central and most of the southern areas (Figure 5c), which are covered mainly by trees, shrubs, and grasslands. Overall, there was no significant change in functional connectivity status in 2010, with a total current of 33.24, compared with 1998, with a total current of 34.18, but the situation was significantly better in 2018, with a total current of 65.83 (Figure 5), especially in regions with increased green areas. As shown in the Figure 5, the area with low current density (i.e., high landscape resistance)

is concentrated in the southeast, which is dominated by construction areas and ore piles, gravel pits, etc., with high human activities that hinder the communication between ecological species, followed by the central northwest corner, which is distributed with water sources, cultivated land, construction areas, etc. The areas with high currents and relatively low resistance were mainly concentrated in Xishan, Yanqing, and Changping Districts, the Baihuashan and Lingshan Biodiversity Reserves, and Mentougou and Fangshan Districts, where human activities were low, further indicating that migration resistance was related to human disturbance.

The potential distribution of ecological corridors can be reflected by the overall connectivity. The comparison of 1998–2018 (Figure 5) reveals that areas with high connectivity are more likely to be restored. We use the natural break method to classify circuit connectivity into levels, and the areas and those counted from 1998–2018 are shown in Figure 6. Mentougou District has the largest area of high connectivity, and Yanqing and Fangshan Districts have larger areas of low connectivity. The Haidian, Yanqing, and Shijingshan areas have very little current passing through, probably related to urban construction and strong human activity.

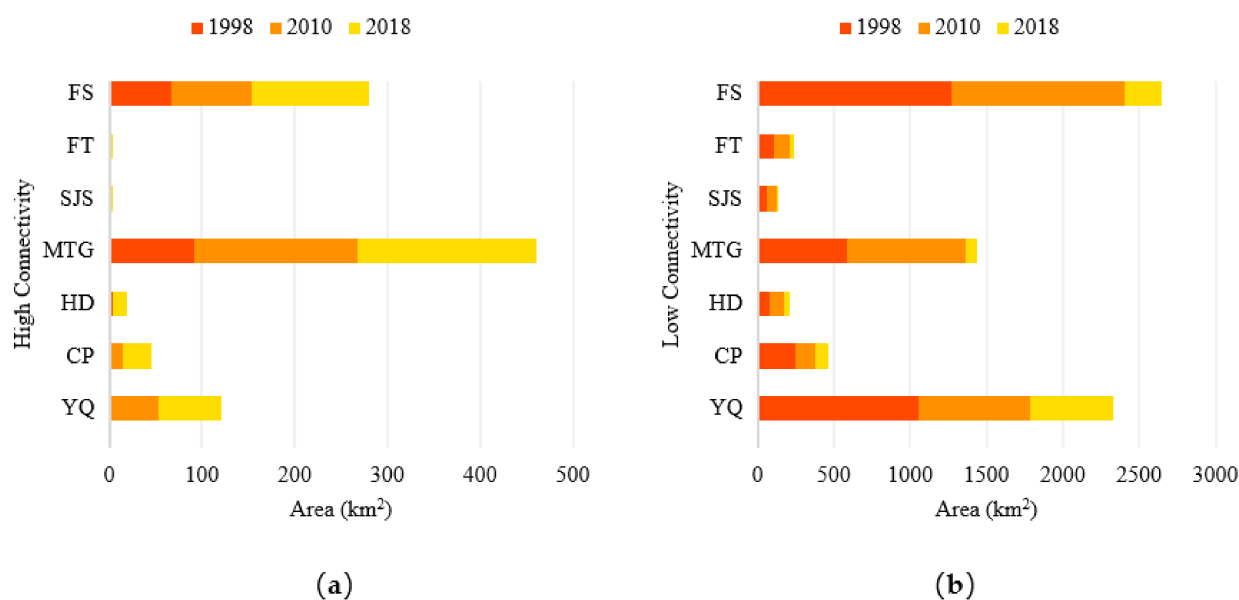


**Figure 6.** Zoning area statistics for high connectivity and low connectivity areas: (a) area of the high current density value region in different zones from 1998–2018; (b) area of the low current density value region in different zones from 1998–2018. In the vertical coordinate, abbreviation FS for Fangshan District; FT for Fangtai District; SJS for Shijingshan District; MTG for Mentougou District; HD for Haidian District; CP for Changping District; and YQ for Yanqing District.

According to the simulation results (Figure 7) of Linkage Pathways, a total of 70, 74, and 152 active least-cost paths and ecological corridors were finally identified in 1998, 2010, and 2018, respectively. The proportion of ecological corridors in the 1–10 km range is gradually increasing, and the ecological corridors are becoming more numerous and shorter. As can be seen from Figure 7, the ecological network is becoming more and more complete and basically covers the entire study area, indicating that the distribution of ecological source sites is becoming more and more rationalized. The inactive LCPs are mainly located around the study area. We used the calculated current flow centrality (which identifies the most important links for maintaining connectivity between networks) to select the top 10 important ecological corridors (>1 km) for analysis [29,40]. In addition, the smaller the ratio of cost-weighted distance to least-cost path distance, the stronger the connectivity of the ecological corridors, which leads to the conclusion that ecological corridors are more critical [29,31]. These corridors are distributed as shown in Figure 7. It can be seen from

Figure 7c that the high centrality corridors are mainly located in the middle and narrow part of the study area, where important mountains and forests are distributed, and play an important role in maintaining ecological network connectivity, which should be an important priority target for biodiversity conservation.

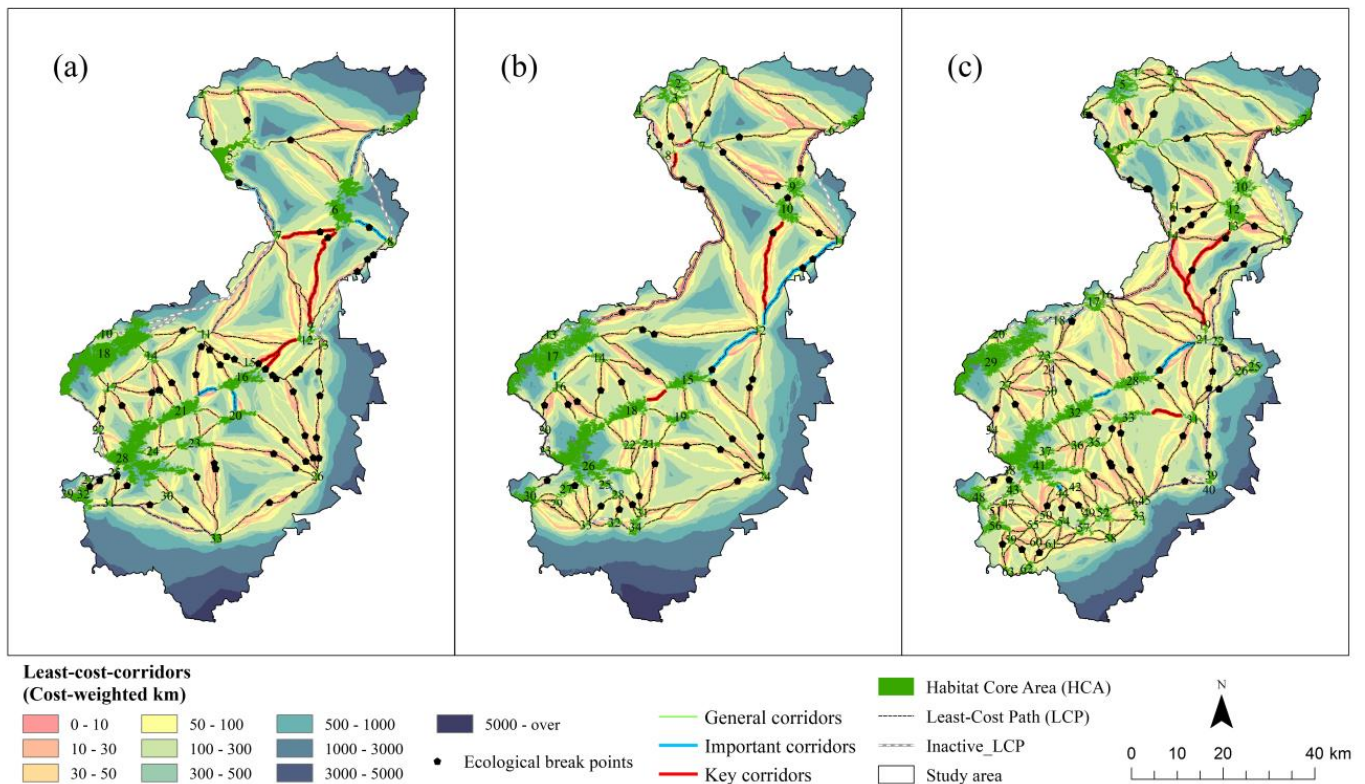


**Figure 7.** Spatial distribution of ecological breakpoints: (a) year 1998; (b) year 2010; and (c) year 2018.

Traffic roads can hinder the communication of organisms. Ecological breakpoints are obtained through the intersection of ecological corridors and traffic roads in Beijing. The distribution locations of the break points are shown in Figure 7, and we obtained, respectively, 51, 44, and 73 ecological breakpoints in 1998, 2010, and 2018. With the improvement of functional connectivity in the study area, the interference of traffic roads with ecological networks and the blockage of ecological corridors gradually increased. Analyzing the number of ecological breakpoints in terms of major traffic road types, 19, 19, and 34 were located on railroads, 2, 1, and 14 on expressways, and 30, 24, and 25 on national highways in 1998, 2010, and 2018, respectively (Table 6). In 2018, the traffic road was well developed in the study area, resulting in the most fragmented habitat corridors, as shown in the Figure 7. Although the corridor connectivity between the central network and the eastern network of the study area has improved over the years due to the construction of riverine protection forests and road forest networks, there is a lack of intermediate nodes. For example, the passage of the railroad in the vicinity of HCA 11 in 1998 (Figure 7a) caused a serious break in the connecting corridor and deepened the habitat fragmentation, resulting in the destruction of the ecological network structure and the loss of intermediate connecting nodes.

**Table 6.** Statistical metrics of ecological corridors and breakpoints.

Year		1998	2010	2018	1998–2018
Active LCPs (strips)		70	74	152	82
Corridor areas (km <sup>2</sup> )		774.63	856.84	1170.50	395.87
Percentage of corridors (%)		15.03	16.63	22.72	7.68
Inactive LCPs (strip)		13	13	22	9
Number of break points		51	44	73	22
Number of breakpoints (by type of road)	Railroad	19	19	34	15
	Expressway	2	1	14	12
	National highway	30	24	25	−5

The top ten least-cost paths for current centrality ranking in 1998, 2010, and 2018 were selected, respectively, for analysis, as shown in Table 7. From the results, it can be found that the maximum values of the first ten currents by centrality, as well as the overall average values, are gradually increasing. These centrality values were particularly high in the associations between HCA 16 and 21 in 1998 (Figure 7a), HCA 12 and 15 in 2010 (Figure 7b), and HCA 28 and 32 in 2018 (Figure 7c). The HCA 16 of 1998, the HCA 15 of 2010, and the HCA 28 of 2018 are all connected with the highest centrality links (Table 7), and the fact that these three core areas are located in one place suggests that the habitat and links in this region play a key role in maintaining connectivity and may provide important stepping stones for connectivity and that any disturbance could disrupt connectivity. The CWD describes how resistance accumulates as it traverses the landscape outward from the HCA. The CWD/LCP represents the average resistance between optimal paths with multiple pairs of LCPs moving relative to each other. When the CWD/LCP values are larger, species suffer greater resistance to migration or dispersal through this least-cost pathway, and the landscape connectivity is poorer. The comparison revealed that links with high centrality may also have large CWD/LCP values (Table 7), such as the link of HCA 16 and 21 in 1998, indicating that species suffer from greater resistance to migration or dispersal through this least-cost pathway, resulting in reduced connectivity, which needs to be protected to maintain the link connectivity levels. When analyzed in conjunction with the land use type map, it was found that most of the paths with high consumption passed through land use types with high resistance surfaces such as built-up areas, bare land, and industrial and mining areas.

Based on the run-out CWD and the size of the habitat core area, we chose 50 km [29] as the corridor width for the ecological corridor, and this width is the size of the cost-weighted distance. The results of calculating the adjacent pair pinch points using Circuitscape are shown in Figure 8; unconstrained to highly constrained areas were allowed to move along the connection. The areas with high current values represent bottlenecks in the corridor and are likely to be the most vulnerable, with a potential risk of separating habitat core areas. The pinch points in 1998 were mainly concentrated in the northwestern and eastern parts of the study area and the perimeter of the habitat (Figure 8a). Compared with 1998, the ecological pinch points in the central and western part of the study area increased significantly in 2010 (Figure 8b), which may be related to the fragmentation of the habitat patches and the deterioration of the surrounding ecological environment. As is shown in the Figure 7a, the large number of pinch points distributed near HCA 11 in 1998, indicates that the water source area plays a key role in landscape connectivity and is vulnerable to damage and loss.

Although the overall connectivity of the study area was greatly improved in 2018 (Figure 8c), the areas of fragile and narrow pinch points became more numerous. The highly restricted pinch points may be due to the expansion of traffic roads and the high-density built-up areas, and the lack of potential low-cost pathways in the vicinity of some link areas.

Despite the potential importance of these pinch points for maintaining the connectivity of the ecological network integrity, however, the narrow nature of these connections means that they are fragile and may not persist with future land use changes. For example, the pinch points between HCA 16 and 12 in 1998 (Figure 8a), HCA 15 and 12 in 2010 (Figure 8b), and HCA 28 and 21 in 2018 (Figure 8c) change significantly as the surrounding land use is strongly disturbed by anthropogenic interference, surrounded mainly by the Yongding River, Miaofeng Mountain Park, Laobadi Scenic Area, and so on. Figure 8 shows that there is a large number of pinch points within the Baihua Mountain Nature Reserve, such as between HCA 18 and 22 (Figure 8a), HCA 17 and 20 (Figure 8b), and HCA 29 and 34 (Figure 8c), and a large number of pinch points also exist in the southern part of the study area (Figure 8). The encroachment of urban development may destroy the already weak connectivity and further reduce the “pinch points”; so, the pinch point area should be a priority area to protect the connectivity.

**Table 7.** Characteristics of the 10 current flow centralities sorted by decreasing order.

Year	Habitat Core Areas (A–B) <sup>1</sup>	Cost-Weighted Distance (CWD) (m)	LCP Distance (m)	CWD/LCP <sup>2</sup>	Current Flow Centrality (amps)
1998	16–21	1,243,684.9	4751	261.77	94.8
	12–13	254,030.9	1215	209.08	84.1
	16–20	1,288,180.4	4556	282.74	68.6
	4–6	3,358,211.3	13,473	249.25	62.3
	12–16	2,366,038.0	10,306	229.58	60.1
	5–7	4,711,881	16,202	290.82	59.8
	12–15	2,550,988.3	10,824	235.68	55.5
	6–9	5,611,562	23,819	235.59	53.5
	6–7	2,801,278.8	12,230	229.05	52.8
	6–8	2,008,986.6	8425	238.46	50.8
2010	12–15	3,287,091.3	15,107	217.59	111.4
	10–12	5,363,715	25,300	212.00	83.6
	25–28	292,513.3	1190	245.81	76.6
	16–17	423,946.3	1744	243.09	72.7
	14–17	319,338.9	1332	239.74	70.7
	15–18	1,085,680.1	5108	212.55	70.2
	7–8	564,652.9	3947	143.06	69.1
	6–9	2,714,221.5	13,432	202.07	67.7
	11–12	6,246,280	27,155	230.02	66.1
	8–17	13,488,987	65,391	206.28	65.6
2018	28–32	813,206.4	4214	192.98	234.4
	17–18	1,117,795	5485	203.79	224.2
	14–16	3,962,851	2,3101	171.54	219.9
	18–29	467,855.4	2256	207.38	187.0
	14–19	3,389,893.5	22,811	148.61	185.8
	21–28	2,262,608.5	12,000	188.55	183.0
	31–33	1,259,569	7282	172.97	177.9
	8–10	2,232,187	13,236	168.65	173.6
	13–19	4,281,318.5	28,036	152.71	172.3
	41–44	270,386.3	1555	173.88	171.5

<sup>1</sup> A–B indicates the 2 connected HCAs. <sup>2</sup> Provides the resistance per unit of length along least-cost path corridors.

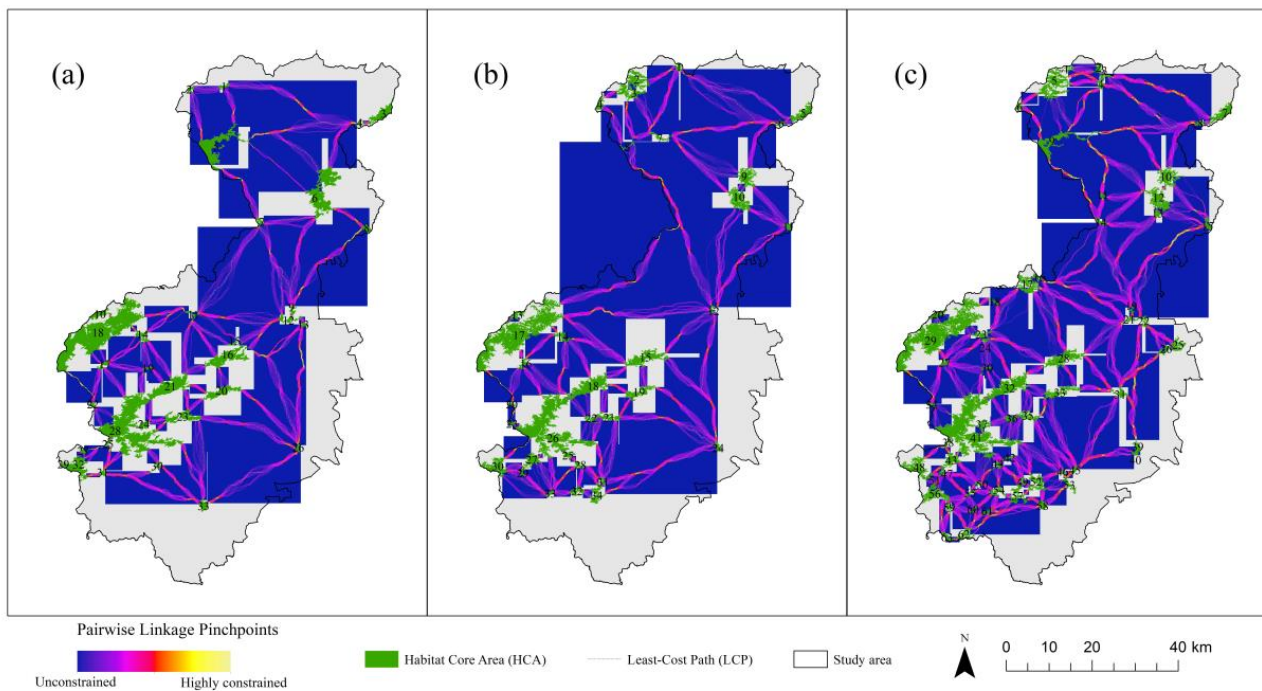


**Figure 8.** The spatial patterns of adjacent pair pinch points and bottleneck areas: (a) year 1998; (b) year 2010; and (c) year 2018.

In order to better maintain and improve landscape connectivity, it is particularly important to precisely identify the barrier zones for making further planning. Considering the heterogeneity of urban areas, in this paper we set a variable search radius of 300–900 m for the identification of barrier areas in the study area. It can be seen from Figure 9 that a total of 11, 14, and 25 barrier points were identified, respectively, in 1998, 2010, and 2018. Overall, most of the high barrier areas were mainly located in the southwest corner of the study area, and gradually increased with the increase in ecological source sites. The barriers with the highest impact scores in 1998 were mainly between HCA 21 and 28 (Figure 9a), linked along the connection line, indicating their potential to significantly improve connectivity; the barriers with the highest impact scores in 2010 were mainly around HCA 27, 29, 30 (Figure 9b), and the barriers with the highest impact scores in 2018 were mainly between HCA 45, 46, and 53 (Figure 9c). The comparison (Figure 9) revealed that in some places, the original barrier areas were restored, and the connectivity was improved. Some new ecological source areas have improved the landscape connectivity of the study area, but there are more obstacle points due to their own conditions as well as those of the unstable surroundings. Fragmented forest core areas show more connectivity issues. As shown in Figure 9a, HCA 6 in 1998 gradually fragmented, which may be related to an unlikely altered state highway and the surrounding traffic roads. The state highway passes between HCA 9 and 10 in 2010 and creates a truncation of the ecological corridor between them, creating high barrier points. The same applies to HCA 10 and 12 (Figure 9c), but the barriers were somewhat repaired in 2018 compared to 2010.

### 3.3. Trend Analysis of Spatial Fragmentation of Corridor Habitats during 1998–2018

A series of irrational human developments and utilization, such as indiscriminate logging, uncontrolled mining, and expansion of built-up areas, leads to a higher degree of spatial fragmentation in the NBECA, which in turn can affect the weakening of biodiversity functions. We calculated the landscape fragmentation index  $F_i$  to reflect the change of fragmentation degree of each landscape type, as was shown in Figure 10. Between 1998 and 2018, the bare land and water fragmentation was the most obvious in the study area, and there was also an overall upward trend in the fragmentation of tree forest,

shrubland, and cropland. The fragmentation of these landscapes is strongly associated with human activities. The fragmentation of built-up areas and mining sites is reduced, and the fragmentation of grasslands is relatively recovered, indicating that construction of urban areas is becoming more concentrated, and the ecological environment of mining sites and grasslands is effectively restored. Among all land use types, the fragmentation of water body patches is the most serious, possibly affecting the spatial distribution pattern of ecological corridors as well as ecological nodes.

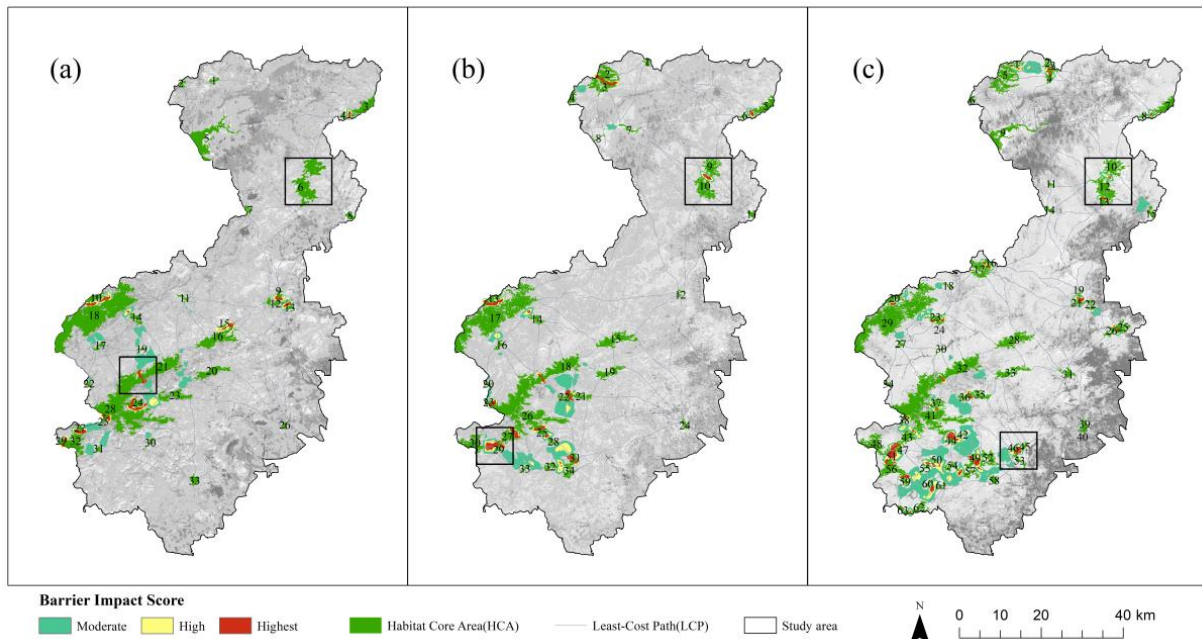


**Figure 9.** The map of barrier impact scores (red or yellow places, if restored or enhanced, may yield greatest improvement to potential connections between habitat core areas; bright green areas, if restored, may yield moderate improvement to potential movement): (a) year 1998; (b) year 2010; and (c) year 2018. The underlying pad of the gray background is, respectively, the resistance surface of different periods.

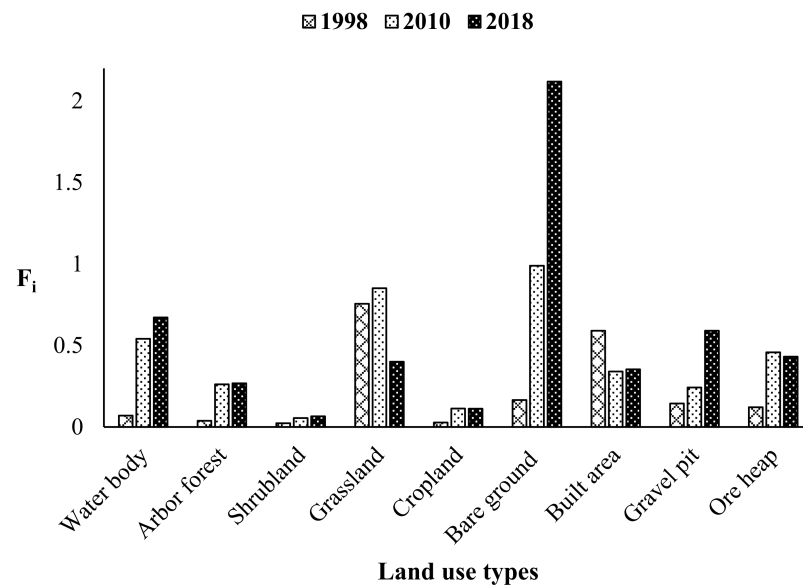


**Figure 10.** Trend chart of landscape fragmentation index ( $F_i$ ).

The changes in land use in the study area from 1998 to 2018 are closely related to the relevant policies and regulations promulgated by the government. For example, the promulgation of “the Beijing Urban Master Plan 2004–2020” actively promoted the construction of green areas and the protection of ecological conservation areas in Beijing, which led to the improvement of forest coverage and the improvement of developed areas with serious ecological damage. During the 12th Five-Year Plan period (2011–2015), Beijing carried out three comprehensive watershed management projects to accelerate the construction of the green ecological development zone of the Yongding River, thereby promoting the development of the waterfront economy in the southwestern region. The ecological service functions of the Yongding River basin, such as wind control and sand fixation, water connotation, soil conservation and climate regulation, have been effectively enhanced.

The trends in the structure and fragmentation of the ecological corridors show that policy changes have an impact on the composition of land use types in the corridor. Negative values in the table indicate a decrease in the share of land use types in the corridor. As is shown in Table 8, the share of arbor forest and shrubland continues to increase while the share of cropland and ore heap continues to decrease. The proportion of both water body and bare ground shows a decreasing trend followed by an increasing trend, while grassland, built-up area, and gravel pit show the opposite trend of increasing followed by decreasing. The composition of land use determines the quality of ecological corridors and the appropriate corridor width. With the possible further fragmentation of ecological corridors, it is important to develop appropriate land use plans for biodiversity conservation.

**Table 8.** Trends in the structure and fragmentation of ecological corridors.

	Land Use Type	1998–2010	2010–2018	1998–2018
The rate of change in the proportion of corridors (%)	Water body	−3.24	0.88	−2.36
	Arbor forest	3.92	1.46	5.38
	Shrubland	0.35	2.97	3.32
	Grassland	0.44	−0.28	0.16
	Cropland	−3.38	−3.81	−7.19
	Bare ground	−0.34	0.01	−0.33
	Built area	2.10	−0.99	1.11
	Gravel pit	0.21	−0.19	0.02
	Ore heap	−0.02	−0.06	−0.08
Landscape fragmentation index		0.04	0.04	0.08

#### 4. Discussion

Analyzing the evolution characteristics of the ecological blockage status of the region based on a time series helps to reveal the mutual influence relationship between human activities and regional ecological functions in nature conservation areas, which is of great significance for promoting the construction of ecological civilization and effectively coordinating the relationship between economic development and ecological environmental protection. In this paper, representative time points are selected to compare the changes. The year 1998 was a period of low economic development and prone to disaster in Beijing, while 2010 to 2018 coincided with the period when Beijing vigorously promoted its conservation policies. Although the interval is different, it still highlights the significantly changed situation.

Our study verified the scientific accuracy and credibility of using the remote sensing ecological index to identify habitat core areas [51,52]. Although the accuracy we obtained is not very high, it still has great potential for application. Firstly, the selection of remote sensing images as the data source is more objective and avoids the subjectivity of human interference; secondly, the remote sensing ecological index includes four indexes, greenness,

wetness, dryness, and heat, which are more comprehensive than a single index table and can effectively identify the core areas of nature reserves with less human interference. The remote sensing ecological index can well describe the quality of the regional ecological environment, and it is more objective to use remote sensing image data for evaluation than other data sources [46].

#### 4.1. Correlation Analysis

Despite the regularity of the decreasing and then increasing ecological sensing index in recent years, the overall ecological sensing index in the study area has continued to develop in a positive direction. In general, the ecological environment quality of the region has been in a good and stable state. The area of high-quality areas increased significantly in 2018, which may be related to the increase in urban green areas in the study area, the return of farmland to forests, and the repair of eco-damaged areas such as gravel pits and ore piles. The results of the circuit model show the level of human impact on habitat connectivity and other ecological flows (e.g., dispersal and gene flow), which is determined by the interaction with the landscape of the intensity of human activities, the temporal span of such activities, the biophysical vulnerability, and, particularly, habitat loss and fragmentation [64]. Pinchpoint Mapper is based on a current flow model derived from circuit theory and can identify pinch points (or bottlenecks), i.e., segments of a link that limit animal movement due to unfavorable land cover, construction, traffic, human disturbance, or a combination of these factors. Ecological pinch points characterize the “necessary paths” in the flow of species, where damage and degradation reduce the connectivity of the ecological network and whose dynamics closely influence the state of the ecological corridor blockage. The most serious fragmentation of water bodies in the northwest ecological connotation area in recent years may be related to the factors of precipitation, climate, and human interference, which cause the separation of water patches and thus the formation of scattered patches. Figure 5 shows that ecological planning in Beijing has yielded significant outcomes in recent years, with the emphasis on ecological protection, the commitment to the planning of the green space system network, and the establishment and planning of the expansion of nature reserves, forest parks, wetlands, and wind and sand management areas, resulting in the effective protection of wildlife and typical ecosystems. By analyzing the evolution of land cover and ecological patterns, we know that land policies, such as reforestation, control of urban development, and the implementation of nature-conservation-related policies and regulations, have the greatest impact on the ecological blockage status of the NBECA. The zones with greater ecological blockage are often located in areas with high anthropogenic disturbance, such as built-up areas, cultivated land, and land destruction areas. Therefore, the approach of remote data analysis in the identification of habitat areas could be useful in land use and land cover detection and prediction research [65,66].

#### 4.2. Suggestions for Improvement and Restoration of Ecological Blockage Conditions

In consideration of the ecological blockage situation in the northwest ecological containment area of Beijing, we propose the restoration proposals of prioritizing the protection of ecological pinch point areas, prioritizing the restoration of ecological barrier point areas, enhancing the maintenance of ecological break point areas, and improving the habitat quality in low ecological quality areas to prevent the continuous deepening of the damage and, for the areas with low overall connectivity, appropriately increasing the green space coverage. For habitat core areas, patches with a high degree of ecological importance should be continuously maintained, and priority should be given to restoring habitat patches that are continuously fragmented and to strengthening the protection of new patches. As for the ecological corridors, in addition to dredging areas that block ecological communication, corridors with high resistance should be maintained and improved, and attention should be paid to those with high fragmentation. Furthermore, we propose a reference scheme for zoning for ecological protection and restoration. As shown in Figure 11, (1) Yanqing Forest

and Ecological Function Maintenance Area; (2) Yanqing Water Containment and Ecological Function Restoration Area; (3) West Hill Soil and Water Conservation Restoration Area; (4) Mentougou Soil and Water Conservation and Forest Restoration Area; (5) Hundred Flowers Mountain-Ling Mountain Biodiversity Reserve; (6) Southern Fangshan Biodiversity Conservation and Forest Restoration Area; (7) Comprehensive Improvement and Ecological Restoration Area: Fengtai; Haidian; Shijingshan and the part of the Fangshan and Changping District.

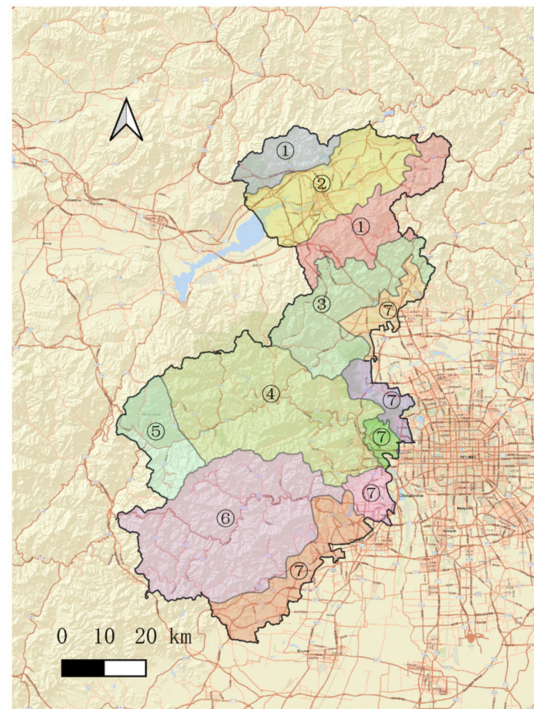


**Figure 11.** Zoning protection and restoration based on the study area.

#### 4.3. Research Limitations and Future Further Research

Due to the complexity and low feasibility of acquiring high-precision data, this study used a large quantity of data at different spatial scales and different resolutions, which may lead to statistical noise from combining data at different spatial scales. More attention needs to be paid to this problem in future studies. We selected arboreal woodlands as well as water patches as habitat core areas for the land use status of the study area and analyzed a blocking change in good forest-water corridors. In this study, we overlook the species information, which made a loss of great significance for the ecological corridors. Follow-up studies should further investigate the selection of focal species and habitat modeling for the conservation areas. In terms of the resistance assignment, we refer to the relevant literature for rank assignment and use the combination weights proposed by experts for weighted superposition of impact factors to obtain the landscape resistance surface of the study area, which is scientific but somewhat subjective. In the future, we should consider the construction of ecological resistance surfaces from a more objective perspective. In this paper, the ecological corridor width is set according to the size and cost-weighted distance of the ecological source sites, without reference to the conservation and migration of specific species, and the physical width of their migration corridors still needs to be studied in depth. Exploring the effective threshold of corridor width will help to build a more scientific and targeted ecological blocking pattern. In addition, from the perspective of ecological services, the Northwest Ecological Containment Area is not an independent system; woodlands, watersheds, and mountains are all interconnected and should be further improved in the future, such as by adding buffer zones at the boundary of

the study area to strengthen the connection with the surrounding ecological environment. The above shortcomings will need further in-depth research in the future.

## 5. Conclusions

This paper takes the northwestern ecological cultured area of Beijing as the study area and analyzes the spatial and temporal patterns of the ecological blockage status of the ecological functional areas in terms of overall connectivity, ecological breakpoints, ecological pinch points, and ecological barrier points based on the circuit theory model and explores the impact of anthropogenic activities on the landscape function and structure of ecological cultured areas, while making a relevant discussion for the changing trend of corridor habitat fragmentation. In addition, specific remediation and optimization suggestions are made based on the land use situation in 2018 in terms of ecological blockage restoration, network maintenance, and protected area management planning. The main conclusions are as follows,

(1) The average RSEIs calculated from the study area were, respectively, 0.65, 0.59, and 0.75 in 1998, 2010, and 2018, indicating that the ecological quality was at a good level and showed a trend of first decreasing and then increasing. The 33, 34, and 63 HCAs with good stability were, respectively, identified by ecological quality and patch importance in 1998, 2010, and 2018 and mainly distributed in the central and southwestern part of the study area. The number of ecological corridors and their shared areas show a gradually increasing trend with the probability of migration in the study area. The 70, 74, and 152 ecological corridors were identified in 1998, 2010, and 2018, respectively. On the whole, the overall connectivity of the study area has improved to some extent with the effectiveness of the comprehensive management of the capital, but some urban areas have been relatively low in connectivity, with relatively strong ecological blockage conditions.

(2) While the corridor ecological break points, ecological pinch points, and barriers increase year by year, the overall positive trend does not mean that all places are positive. In places with many traffic roads, places with many human activities, vulnerable places, etc., the ecological blockage is relatively serious or even worse over time. The increase in the number of ecological breakpoints is related on the one hand to the change in the distribution of the potential corridors and the increase in their number, which is inseparably linked to the increase in connectivity and, on the other hand, to the increase in the number of traffic roads, which seriously affects the biological exchange and requires priority restoration and protection. Ecological pinch points are more concentrated in the central part of Yanqing District. There is a continuous increase in the number of ecological barriers in the southwestern part of the study area, which is inseparable from the increased fragmentation of the forest area. Water fragmentation was the highest among all the habitats, and habitat fragmentation greatly influenced the change of blocking status in the study area. In the future, we should take further restoration and protection measures in response to the blockage status and fragmentation.

**Supplementary Materials:** The following are available online at <https://www.mdpi.com/article/10.3390/rs14051151/s1>, Table S1: Common terms, units and ecological significance in circuit theory. Circuit theory relates circuits to ecology through random wander theory, where the landscape is considered as a conducting surface during biological communication and the probability of migration during random wandering is consistent with the current equation  $I = U/R$  [26]. The regional ecological network is considered as a circuit structure, using the landscape resistance surface as a resistance and running a current through the structure with a constant voltage.

**Author Contributions:** Conceptualization, J.X., J.W. and N.X.; methodology, J.X.; software, J.X. and Y.C.; validation, J.X., L.S. and Y.W.; formal analysis, J.X., L.S., Y.C. and L.A.; investigation, J.X., Y.C., L.S., Y.W. and L.A.; resources, J.W.; data curation, J.X.; writing—original draft preparation, J.X.; writing—review and editing, J.X. and J.W.; visualization, J.X.; supervision, J.W.; project administration, J.X.; funding acquisition, J.W. and N.X. All authors have read and agreed to the published version of the manuscript.

**Funding:** This research was funded by the National Natural Science Foundation of China (42071342, 42171329, 31870713) and the Natural Science Foundation of Beijing, China (8222069, 8222052).

**Institutional Review Board Statement:** Not applicable.

**Informed Consent Statement:** Not applicable.

**Data Availability Statement:** Not applicable.

**Acknowledgments:** We are grateful to the undergraduate students and staff of the Laboratory of Forest Management and “3S” technology, Beijing Forestry University.

**Conflicts of Interest:** The authors declare no conflict of interest. The funders had no role in the design of the study; in the collection, analyses, or interpretation of data; in the writing of the manuscript; or in the decision to publish the results.

## References

- Fahrig, L. Effects of Habitat Fragmentation on Biodiversity. *Annu. Rev. Ecol. Evol. Syst.* **2003**, *34*, 487–515. [[CrossRef](#)]
- Krauss, J.; Bommarco, R.; Guardiola, M.; Heikkinen, R.K.; Helm, A.; Kuussaari, M.; Lindborg, R.; Öckinger, E.; Pärtel, M.; Pino, J.; et al. Habitat fragmentation causes immediate and time-delayed biodiversity loss at different trophic levels. *Ecol. Lett.* **2010**, *13*, 597–605. [[CrossRef](#)]
- Cheng, C.; Hu, Y.; Zhao, M. Progress and prospect of the spatiotemporal change and ecosystem services evaluation of urban green space pattern. *Prog. Geogr.* **2020**, *39*, 1770–1782. [[CrossRef](#)]
- LaPoint, S.; Balkenhol, N.; Hale, J.; Sadler, J.; van der Ree, R. Ecological connectivity research in urban areas. *Funct. Ecol.* **2015**, *29*, 868–878. [[CrossRef](#)]
- Andrén, H. Effects of Habitat Fragmentation on Birds and Mammals in Landscapes with Different Proportions of Suitable Habitat: A Review. *Oikos* **1994**, *71*, 355–366. [[CrossRef](#)]
- Goodwin, B.J. Is landscape connectivity a dependent or independent variable? *Landscape Ecol.* **2003**, *18*, 687–699. [[CrossRef](#)]
- Bednar, M.; Sarapatka, B.; Mazalova, M.; Kuras, T. Connectivity modelling with automatic determination of landscape resistance values. A new approach tested on butterflies and burnet moths. *Ecol. Indic.* **2020**, *116*, 106480. [[CrossRef](#)]
- Saura, S.; Bertzky, B.; Bastin, L.; Battistella, L.; Mandrici, A.; Dubois, G. Global trends in protected area connectivity from 2010 to 2018. *Biol. Conserv.* **2019**, *238*, 108183. [[CrossRef](#)]
- Su, J.; Yin, H.; Kong, F. Ecological networks in response to climate change and the human footprint in the Yangtze River Delta urban agglomeration, China. *Landsc. Ecol.* **2020**, *36*, 2095–2112. [[CrossRef](#)]
- Pelorusso, R.; Gobattoni, F.; Geri, F.; Monaco, R.; Leone, A. Evaluation of Ecosystem Services related to Bio-Energy Landscape Connectivity (BELC) for land use decision making across different planning scales. *Ecol. Indic.* **2016**, *61*, 114–129. [[CrossRef](#)]
- Pierik, M.E.; Dell’Acqua, M.; Confalonieri, R.; Bocchi, S.; Gomasca, S. Designing ecological corridors in a fragmented landscape: A fuzzy approach to circuit connectivity analysis. *Ecol. Indic.* **2016**, *67*, 807–820. [[CrossRef](#)]
- McRae, B.H.; Beier, P. Circuit theory predicts gene flow in plant and animal populations. *Proc. Natl. Acad. Sci. USA* **2007**, *104*, 19885–19890. [[CrossRef](#)] [[PubMed](#)]
- Minor, E.S.; Urban, D.L. A Graph-Theory Framework for Evaluating Landscape Connectivity and Conservation Planning. *Conserv. Biol.* **2008**, *22*, 297–307. [[CrossRef](#)] [[PubMed](#)]
- Monteiro, A.T.; Fava, F.; Gonçalves, J.; Huete, A.; Gusmeroli, F.; Parolo, G.; Spano, D.; Bocchi, S. Landscape context determinants to plant diversity in the permanent meadows of Southern European Alps. *Biodivers. Conserv.* **2013**, *22*, 937–958. [[CrossRef](#)]
- Nikolakaki, P. A GIS site-selection process for habitat creation: Estimating connectivity of habitat patches. *Landsc. Urban. Plann.* **2004**, *68*, 77–94. [[CrossRef](#)]
- Schmitt, T.; Varga, Z.; Seitz, A. Forests as dispersal barriers for *Erebia medusa* (Nymphalidae, Lepidoptera). *Basic Appl. Ecol.* **2000**, *1*, 53–59. [[CrossRef](#)]
- Lande, R. Genetics and Demography in Biological Conservation. *Science* **1988**, *241*, 1455–1460. [[CrossRef](#)]
- Qu, R.; Hou, L.; Lü, H.; Li, H. The gene flow of population genetic structure. *Hereditas* **2004**, *26*, 377–382. [[CrossRef](#)]
- Trizio, I.; Crestanello, B.; Galbusera, P.; Wauters, L.A.; Tosi, G.; Matthysen, E.; Hauffe, H.C. Geographical distance and physical barriers shape the genetic structure of Eurasian red squirrels (*Sciurus vulgaris*) in the Italian Alps. *Mol. Ecol.* **2005**, *14*, 469–481. [[CrossRef](#)]
- Vignieri, S.N. Streams over mountains: Influence of riparian connectivity on gene flow in the Pacific jumping mouse (*Zapus trinotatus*). *Mol. Ecol.* **2005**, *14*, 1925–1937. [[CrossRef](#)]
- Keller, I.; Nentwig, W.; Largiadér, C.R. Recent habitat fragmentation due to roads can lead to significant genetic differentiation in an abundant flightless ground beetle. *Mol. Ecol.* **2004**, *13*, 2983–2994. [[CrossRef](#)] [[PubMed](#)]
- Vos, C.C.; Chardon, J.P. Effects of habitat fragmentation and road density on the distribution pattern of the moor frog *Rana arvalis*. *J. Appl. Ecol.* **1998**, *35*, 44–56. [[CrossRef](#)]
- Purrenhage, J.L.; Niewiarowski, P.H.; Moore, F.B.G. Population structure of spotted salamanders (*Ambystoma maculatum*) in a fragmented landscape. *Mol. Ecol.* **2009**, *18*, 235–247. [[CrossRef](#)] [[PubMed](#)]

24. Ning, Y.; Wang, Y.F.; Li, X.X.; Ma, J.C. Analysis of the application potential of circuit theory in plant landscape genetics. *Plant. Sci. J.* **2019**, *37*, 116–123. [[CrossRef](#)]
25. McRae, B.H. Isolation by resistance. *Evolution* **2006**, *60*, 1551–1561. [[CrossRef](#)]
26. McRae, B.; Dickson, B.; Keitt, T.; Shah, V. Using circuit theory to model connectivity in ecology, evolution, and conservation. *Ecology* **2008**, *89*, 2712–2724. [[CrossRef](#)] [[PubMed](#)]
27. Wu, Y.; Wu, J.; Bi, X.; Li, Y.; Xiao, L. Application of the least cost distance model and the circuit theory model in the evaluation of wetland landscape connectivity in the Yellow River Delta. *Acta Ecol. Sin.* **2022**, *42*, 4. [[CrossRef](#)]
28. Dickson, B.G.; Albano, C.M.; Anantharaman, R.; Beier, P.; Fargione, J.; Graves, T.A.; Gray, M.E.; Hall, K.R.; Lawler, J.J.; Leonard, P.B.; et al. Circuit-theory applications to connectivity science and conservation. *Conserv. Biol.* **2019**, *33*, 239–249. [[CrossRef](#)] [[PubMed](#)]
29. Kong, F.; Wang, D.; Yin, H.; Dronova, I.; Fei, F.; Chen, J.; Pu, Y.; Li, M. Coupling urban 3-D information and circuit theory to advance the development of urban ecological networks. *Conserv. Biol.* **2021**, *35*, 1140–1150. [[CrossRef](#)]
30. Song, L.; Qin, M. Identification of ecological corridors and its importance by integrating circuit theory. *Chin. J. Appl. Ecol.* **2016**, *27*, 3344–3352. [[CrossRef](#)]
31. Du, Y.Y.; Wang, Z.Q.; Yu, Q.H.; Yang, Y.C.; Zhang, Q.W. Construction of a regional ecological security pattern based on a habitat quality model and circuit theory: A case study of the Qinling Mountains (Shaanxi Section). *J. Agric. Resour. Environ.* **2021**. [[CrossRef](#)]
32. Liu, J.; Yin, H.; Kong, F.; Li, M. Structure optimization of circuit theory-based green infrastructure in Nanjing. *Acta Ecol. Sin.* **2018**, *38*, 4363–4372. [[CrossRef](#)]
33. Peng, J.; Li, H.; Liu, Y.; Hu, Y.; Yang, Y. Identification and optimization of ecological security pattern in Xiong'an New Area. *Acta Geogr. Sin.* **2018**, *73*, 701–710. [[CrossRef](#)]
34. Yang, Z.G.; Jiang, Z.Y.; Guo, C.X.; Yang, X.J.; Xu, X.J.; Li, X.; Hu, Z.M.; Zhou, H.Y. Construction of ecological network using morphological spatial pattern analysis and minimal cumulative resistance models in Guangzhou City, China. *Chin. J. Appl. Ecol.* **2018**, *29*, 3367–3376. [[CrossRef](#)]
35. Wang, X.Y.; Chen, T.Q.; Feng, Z.; Wu, K.N.; Lin, Q. Construction of ecological security pattern based on boundary analysis: A case study on Jiangsu Province. *Acta Ecol. Sin.* **2020**, *40*, 3375–3384. [[CrossRef](#)]
36. Zhu, Z.J.; Zuo, L.J.; Zhang, Z.X.; Wang, Y.F.; Sun, F.F.; Pan, T.S.; Zhao, X.L.; Wang, X. Analysis of spatial and temporal changes of regional ecological pattern in the northwest of Jingjinji as water conservation area during the past 30 years. *Pratac. Sci.* **2020**, *37*, 1325–1336. [[CrossRef](#)]
37. Niu, W.; Xiao, L.X.; Li, J.X. The North West of Hebei ecological protection and improvement construction strategy based on the perspective of the coordinated development of Beijing-Tianjin-Hebei. *Chin. J. Agric. Resour. Reg. Plann.* **2016**, *37*, 87–92. [[CrossRef](#)]
38. Sun, F.; Zhang, Z.; Zuo, L.; Zhao, X.; Pan, T.; Zhu, Z.; Wang, X.; Liu, F.; Yi, L.; Wen, Q.; et al. Difference assessment on ecological functions of artificial coniferous forests in water conservation area of Northwestern Hebei. *J. Nat. Resour.* **2020**, *35*, 06001348. [[CrossRef](#)]
39. Zhang, Q.; Li, F.; Wang, D.; Li, M. Analysis on changes of ecological spatial connectivity in Jiangsu Province based on ecological network. *Acta Ecol. Sin.* **2021**, *41*, 3007–3020. [[CrossRef](#)]
40. Wang, G.; Bai, W.; Xiong, X.; Mu, X.; Qiu, L. Research on ecological space damage identification of Beijing-Tianjin-Hebei urban Agglomeration. *City Plan. Rev.* **2021**, *8*, 1002–1329. [[CrossRef](#)]
41. Albert, C.H.; Rayfield, B.; Dumitru, M.; Gonzalez, A. Applying network theory to prioritize multispecies habitat networks that are robust to climate and land-use change. *Conserv. Biol.* **2017**, *31*, 1383–1396. [[CrossRef](#)] [[PubMed](#)]
42. Cao, Y.; Yang, R.; Carver, S. Linking wilderness mapping and connectivity modelling: A methodological framework for wildland network planning. *Biol. Conserv.* **2020**, *251*, 108679. [[CrossRef](#)]
43. Delmas, E.; Besson, M.; Brice, M.H.; Burkle, L.A.; Dalla Riva, G.V.; Fortin, M.J.; Gravel, D.; Guimaraes, P.R., Jr.; Hembry, D.H.; Newman, E.A.; et al. Analysing ecological networks of species interactions. *Biol. Rev. Camb. Philos. Soc.* **2018**, *94*, 16–36. [[CrossRef](#)] [[PubMed](#)]
44. Tatem, A.J. WorldPop, open data for spatial demography. *Sci. Data* **2017**, *4*, 170004. [[CrossRef](#)]
45. Xu, H.Q. A remote sensing urban ecological index and its application. *Acta Ecol. Sin.* **2013**, *33*, 7853–7862. [[CrossRef](#)]
46. Xu, H. A remote sensing index for assessment of regional ecological changes. *China Environ. Sci.* **2013**, *33*, 889–897. [[CrossRef](#)]
47. Yang, K.; Lu, Y.; Weng, Y.; Wei, L. Dynamic monitoring of ecological and environmental quality of the Nanliu River basin, supported by Google Earth Engine. *J. Agric. Resour. Environ.* **2021**, *38*, 1112–1121. [[CrossRef](#)]
48. Chen, W.; Huang, H.P.; Tian, Y.C.; Du, Y.Y. Monitoring and assessment of the eco-environment quality in the Sanjiangyuan region based on Google Earth Engine. *J. Geo-Inf. Sci.* **2019**, *21*, 1382–1391. [[CrossRef](#)]
49. Wang, Y.; Zhao, Y.H.; Wu, J.S. Dynamic monitoring of long time series of ecological quality in urban agglomerations using Google Earth Engine cloud computing: A case study of the Guangdong-Hong Kong-Macao Greater Bay Area, China. *Acta Ecol. Sin.* **2020**, *40*, 8461–8473. [[CrossRef](#)]
50. Chen, X.; Zeng, X.; Zhao, C.; Qiu, R.; Zhang, L.; Hou, X.; Hu, X. The ecological effect of road network based on remote sensing ecological index: A case study of Fuzhou City, Fujian Province. *Acta Ecol. Sin.* **2021**, *41*, 4732–4745. [[CrossRef](#)]
51. Wen, X.; Zhou, Z.; Zhang, M.; Zhang, P.; Zhang, G.; Zhang, Q. Identification of Key Areas of Land Space Ecological Restoration in Taihang Mountains—A case study of Tang County. *Chin. J. Eco-Agric.* **2021**, *29*, 2093–2106. [[CrossRef](#)]

52. Lü, D.W.; Cai, H.S.; Zhang, X.L.; Luo, H.L.; Zeng, H.; Zhang, T. Construction and optimization of the ecological security system in Yiyang County based on the remote sensing ecological index. *Res. Agric. Mod.* **2021**, *42*, 545–556. [[CrossRef](#)]
53. Ermida, S.L.; Soares, P.; Mantas, V.; Göttsche, F.M.; Trigo, I.F. Google Earth Engine Open-Source Code for Land Surface Temperature Estimation from the Landsat Series. *Remote Sens.* **2020**, *12*, 1471. [[CrossRef](#)]
54. Xu, H.; Wang, M.; Shi, T.; Guan, H.; Lin, Z. Prediction of ecological effects of potential population and impervious surface increases using a remote sensing based ecological index (RSEI). *Ecol. Indic.* **2019**, *93*, 730–740. [[CrossRef](#)]
55. Anantharaman, R.; Hall, K.; Shah, V.B.; Edelman, A. Circuitscape in Julia: High Performance Connectivity Modelling to Support Conservation Decisions. *JuliaCon Proc.* **2020**, *1*, 58. [[CrossRef](#)]
56. McRae, B.H.; Kavanagh, D.M. *Linkage Mapper Connectivity Analysis Software*; The Nature Conservancy in Washington: Seattle, WA, USA, 2011. Available online: <https://linkagemapper.org> (accessed on 23 October 2021).
57. Meng, J.; Wang, X.; You, N.; Zhu, L. Dynamic changes of landscape connectivity for ecological lands and distance thresholds in the middle reaches of the Heihe River, Northwest China. *Chin. J. Appl. Ecol.* **2016**, *27*, 1715–1726. [[CrossRef](#)]
58. McRae, B.H. *Centrality Mapper Connectivity Analysis Software*; The Nature Conservancy in Washington: Seattle, WA, USA, 2012. Available online: <https://linkagemapper.org> (accessed on 23 October 2021).
59. McRae, B.H. *Pinchpoint Mapper Connectivity Analysis Software*; The Nature Conservancy in Washington: Seattle, WA, USA, 2012. Available online: <https://linkagemapper.org> (accessed on 23 October 2021).
60. McRae, B.H. *Barrier Mapper Connectivity Analysis Software*; The Nature Conservancy in Washington: Seattle, WA, USA, 2012. Available online: <https://linkagemapper.org> (accessed on 23 October 2021).
61. Chen, C.; Wu, S.J.; Douglas, M.C.; Lü, M.Q.; Wen, Z.F.; Jiang, Y.; Chen, J.L. Effects of changing cost values on landscape connectivity simulation. *Acta Ecol. Sin.* **2015**, *35*, 7367–7376. [[CrossRef](#)]
62. Li, H.; Liu, Y.; Li, Q.; Wang, X. Analysis of ecological security pattern of southern rare earth mining area based on MCR model. *Sci. Geogr. Sin.* **2020**, *40*, 989–998. [[CrossRef](#)]
63. Gao, Y.; Liu, Y.X.; Qian, J.L.; Guo, Y.; Hu, Y.S. Improving ecological security pattern based on the integrated observation of multiple source data: A case study of Wannian County, Jiangxi Province. *Resour. Sci.* **2020**, *42*, 2010–2021. [[CrossRef](#)]
64. Ayram, C.A.C.; Mendoza, M.E.; Etter, A.; Salicrup, D.R.P. Anthropogenic impact on habitat connectivity: A multidimensional human footprint index evaluated in a highly biodiverse landscape of Mexico. *Ecol. Indic.* **2017**, *72*, 895–909. [[CrossRef](#)]
65. Rana, M.S.; Sarkar, S. Prediction of urban expansion by using land cover change detection approach. *Heliyon* **2021**, *7*, e08437. [[CrossRef](#)] [[PubMed](#)]
66. Wang, T.; Kazak, J.; Han, Q.; de Vries, B. A framework for path-dependent industrial land transition analysis using vector data. *Eur. Plann. Stud.* **2019**, *27*, 1391–1412. [[CrossRef](#)]